

Friction Stir Processed Advanced Composite Prepared Via Utilizing Industrial Waste

Saurabh¹ and Dr. Puneet katyal²

¹Research Scholar, Department of Mechanical Engineering, Guru Jambheshwar University of Science & Technology, Hisar, Haryana, India

²Associate Professor, Department of Mechanical Engineering, Guru Jambheshwar University of Science & Technology, Hisar, Haryana, India

¹Corresponding Author: saurabhsinghpawar48@gmail.com

Received: 25-04-2023

Revised: 15-05-2023

Accepted: 31-05-2023

ABSTRACT

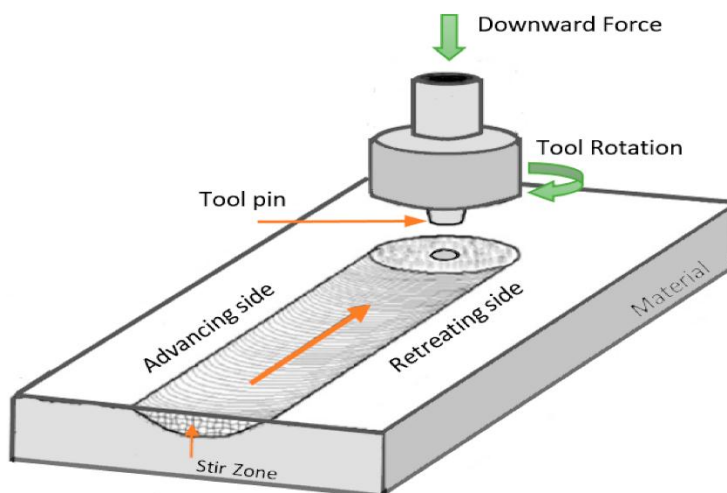
The utilization of magnesium-based composites prepared via FSP and incorporating Fly Ash offers improved mechanical properties, lightweight nature, environmental sustainability, cost-effectiveness, and enhanced thermal and corrosion resistance. These advantages make them highly valuable for a range of industries, promoting their utilization and potential for innovative applications.

Keywords: green house gases, global environment, transport sector, industries, friction stir processing

I. BACKGROUND

The increasing concentration of greenhouse gases (GHG) including carbon dioxide, nitrous oxide (NO), and methane in the atmosphere is to blame for the changing global environment. The transport sector typically accounts for the majority of GHG emissions. According to research, reducing the weight of the vehicle is an effective approach to reducing carbon dioxide emissions in addition to improving aerodynamics, accessories, drive efficiency, and tire rolling resistance (Elalem, A. and El-Bourawi, M. (2010).

Figure 1: Friction stir processing



The demand for the production of lightweight materials has increased significantly over the past few decades in order to build light cars and reduce the emission of these GHG. In contrast to the aforementioned, improving fuel efficiency and giving a vehicle's strength-to-weight ratio is still a significant problem in the transportation business. In order to be used to their full potential, these materials must now have high strength-to-weight ratios and low densities. These standards increase the need for the creation of new lightweight materials with sufficient strength to fulfil contemporary needs.

II. RESULTS & DISCUSSIONS (METALLURGICAL & MECHANICAL)

The base's average grain size was about 75 μm . This is caused by the absence of carbon at all levels in magnesium and its alloys. The spectrograph shows that all of the magnesium component parts of AZ91 are present and that no carbon element is present in the base matrix. The optical micrographs of the magnesium metal composite, created at 1200 rpm and two FSP passes. The friction stir zone (SZ), the thermomechanical affected zone (TMAZ), the heat affected zone (HAZ), and the interface zone (IZ) are all shown in the cross-sectional view of the typical FSPed AZ91/FA Ash nanocomposite in the figure. According to the study of the stir zone, dynamic recrystallization is the main phenomenon. The specimen demonstrates that large grains of magnesium broke up into smaller grains when subjected to the forceful operation of a tool. Finer and coarser grains were present in the stir zone (SZ), creating a heterogeneous microstructural characteristic.

2.1 Effect of FSP Pass Number

- Agglomeration and clustering of nanoparticles in FSP processes are major problems that must be overcome since they have a negative impact on composite strength.
- Every FSP pass creates an additional composite layer on top of the previous one, expanding the processed region.
- Multi-pass FSP helps to reduce n-Fly Ash particulate clusters and promotes uniform reinforcement particle distribution (Zohoor et al., 2012). It thus reduces the matrix's grain size.
- As the number of FSP passes increased, four higher grain boundaries became available.

According to (Bauri et al., 2011), this increase with each FSP pass causes dislocations to form in the grains, and at the same time, high stacking fault energy (SFE) of magnesium causes the creation and dynamic recovery of low-angle sub-grain boundaries. Clusters of very small-sized Fly Ash particles were seen at the tool rotation speed of 1200 rpm and the fourth FSP run as the FSP parameters changed. Less FSP numbers may be to blame for this. It was found that the frictional heat produced at 1200 rpm and after two FSP passes was insufficient to disperse clusters. After two FSP passes, also there was an uneven distribution of Fly Ash particles into the AZ91 matrix. This was further validated by a FESEM study, as shown in Agglomeration of nanoparticles significantly decreases when the FSP pass number is increased to FSP pass 3 while maintaining the same tool rotation speed.

The stress-strain graph of the base material represents the mechanical response of the base material used in the composite. It typically exhibits a linear elastic region followed by a plastic region. In the linear elastic region, the material deforms elastically, and the stress is directly proportional to the applied strain. The graph shows a straight line with a positive slope. Beyond the elastic limit, the material enters the plastic region, where permanent deformation occurs. The stress-strain curve in this region exhibits strain hardening, meaning the material becomes harder to deform as the strain increases. The stress-strain graph for the unreinforced composite refers to the composite material without any additional reinforcement. In comparison to the base material, the composite may exhibit improved mechanical properties. The graph may show a similar initial linear elastic region, but the modulus of elasticity might be slightly different due to the presence of the matrix material. The plastic region may also display enhanced strain hardening, which can be attributed to the interaction between the matrix and the reinforcement.

The stress-strain graph for the AZ91/FA/2 pass FSPed composite represents the composite material produced by subjecting the AZ91 alloy matrix to friction stir processing (FSP) with FA (Fly Ash) reinforcement for two passes. FSP is a solid-state processing technique that can refine the microstructure and improve the mechanical properties of the material. The graph may exhibit a similar initial linear elastic region as the unreinforced composite, but with a higher modulus of elasticity due to the strengthening effect of the FA reinforcement. The plastic region may show further strain hardening, indicating improved ductility and resistance to deformation compared to the unreinforced composite.

The remainder of the nanoparticles on the surface of the base metal were then clumped together and swirled into the base metal. Because of this, nanoparticles did not scatter well and accumulated in significant quantities in the SZ. This also means that some local clustering is unavoidable and that some nanoparticles cannot completely stop grain boundary movement. The reinforcements would consistently assemble in the SZ in large numbers after two runs of composite manufacturing by FSP. In comparison to 1200 rpm and 2 FSP passes, it was observed that grain size and agglomeration of Fly Ash particles were marginally reduced at 1200 rpm and 3 FSP passes. The grain size in SZ has been significantly reduced, or by almost one third to the basic metal. Additionally, Fly Ash particles anchored the grain boundary in addition to the reinforcement particles dispersing in the SZ in a scattered and uniform manner.

The stress-strain graph for the AZ91/FA/3 pass FSPed composite represents the composite material produced by subjecting the AZ91 alloy matrix to friction stir processing with FA reinforcement for three passes. With an additional pass of FSP, the graph may exhibit further improvements in mechanical properties compared to the 2 pass FSPed composite. The

modulus of elasticity might increase, indicating increased stiffness, while the plastic region may show enhanced strain hardening, suggesting improved strength and ductility. The composite exhibit a higher ultimate tensile strength and strain compared to the previous configurations.

III. CONCLUSIONS

In the present work, the focus was on performing Friction Stir Processing (FSP) on the AZ91 Mg alloy and creating surface composites by incorporating reinforcement particles such as Fly ash (FA). The objective was to enhance the metallurgical and mechanical properties of the alloy compared to its as-received state. The research also aimed to investigate the influence of various process parameters and reinforcement particles on these properties.

The following results were obtained from this research:

- 1) FSP led to the formation of a homogeneous microstructure with uniformly dispersed reinforcing particles.
- 2) Due to the vigorous stirring action of the FSP tool during the process, Fly ash particles were evenly distributed within the stir zone.
- 3) The surface composites (AZ91/FA) exhibited significant microstructural refinement compared to the base material.
- 4) Hard Fly ash particles had a greater impact on grain size and hardness in the surface composites compared to unreinforced AZ91 base substrate.
- 5) The use of a triangular tool pin geometry resulted in a greater reduction in grain size.

REFERENCES

1. Lathabai, Sri. (2010). Joining of aluminum and its alloys. *Fundamentals of Aluminum Metallurgy: Production, Processing and Applications*. 607-654. 10.1533/9780857090256.3.607.
2. Cui GR, Ma ZY, Li SX. (2008). Periodical particle flow pattern in friction stir processed Al-Mg alloy. *Scr Mater* 58: 1082–1085.
3. Wang, X. J. et al. (2014). Processing, microstructure and mechanical properties of micro-SiC particles reinforced magnesium matrix composites fabricated by stir casting assisted by ultrasonic treatment processing[†], *Materials and Design*, 57, pp. 638–645. doi: 10.1016/j.matdes.2014.01.022.
4. Wang, L., Xie, L., Shen, P., Fan, Q., Wang, W., Wang, K., Zhang, L.-C. (2019). Surface microstructure and mechanical properties of Ti-6Al-4V/Ag nanocomposite prepared by FSP. *Materials Characterization*, 153, 175–183. doi:10.1016/j.matchar.2019.05.002
5. Wang X, Jha A, Brydson R (2004). In situ fabrication of Al₃ Ti particle reinforced aluminium alloy metal-matrix composites. *Mater Sci Eng A* 364: 339–345.
6. Elalem, A. and El-Bourawi, M. (2010). Reduction of Automobile Carbon Dioxide Emissions[†], *International Journal of Material Forming*, 3, 663–666, doi: 10.1007/s12289-010-0857-2.
7. Kulekci, M.K. (2008). Magnesium and its alloys applications in automotive industry. *The International Journal of Advanced Manufacturing Technology*, 39(9), 851–865, doi: 10.1007/s00170-007-1279-2.